Received: 24 April 2022 | Revised: 30 August 2022 | Accepted: 21 October 2022

DOI: 10.1002/mgg3.2083

Molecular Genetics & Genomic Medicine Open Access WILEY

CLINICAL REPORT

A novel splicing variant of *VCAN* identified in a Chinese family initially diagnosed with familial exudative vitreoretinopathy

Junwei Zhong[1] | **Jie Shi**[1] | **Xiaotian Zhang**[2,3,4] | **Ke Xu**[1] | **Xiaohui Zhang**[1] | **Yue Xie**[1] | **Yang Li**[1]

[1]Beijing Institute of Ophthalmology, Beijing Tongren Eye Center, Beijing Ophthalmology & Visual Sciences Key Lab, Beijing Tongren Hospital, Capital Medical University, Beijing, China

[2]Clinical College of Ophthalmology, Tianjin Medical University, Tianjin, China

[3]Nankai University Eye Hospital, Tianjin, China

[4]Tianjin Key Laboratory of Ophthalmology and Visual Science, Tianjin Eye Hospital, Tianjin, China

Correspondence
Yang Li, Beijing Institute of Ophthalmology, Beijing Tongren Eye Center, Beijing Ophthalmology & Visual Sciences Key Lab, Beijing Tongren Hospital, Capital Medical University, Hougou Lane 17, Chong Nei Street, Beijing 100730, China.
Email: yilbio@163.com

Funding information
the National Key R&D Program of China, Grant/Award Number: 2016YFC0905200

Abstract

Background: Wagner vitreoretinopathy (WVR) is a rare autosomal dominant vitreoretinopathy caused by pathogenic variants in the *VCAN* gene. The aim of this study was to report a novel splicing variant in *VCAN* identified in a three-generation Chinese family initially diagnosed with familial exudative vitreoretinopathy and to describe the patients' clinical features.

Methods: Four affected individuals from a three-generation family underwent detailed ophthalmic examinations, including best-corrected visual acuity by Snellen E chart, slit-lamp biomicroscopy, indirect ophthalmoscopy under pupil dilatation, ocular B-ultrasonography, optical coherence tomography scans, and fundus autofluorescence. Targeted next-generation sequencing was performed to identify variants of the disease-causing gene for the proband, followed by co-segregation analysis using Sanger-DNA sequencing. Reverse transcriptase-polymerase chain reaction (RT-PCR) was carried out to verify the effects of a variant on *VCAN* pre-mRNA splicing in the lymphocytes from the patients.

Results: We detected a novel heterozygous variant c.4004-4_c.4004-3delinsCA of *VCAN* in all four affected individuals. RT-PCR revealed that the novel variant caused an abnormal splicing in exon 8 of the *VCAN* and imbalanced versican transcripts. All four patients presented vitreous syneresis and bilateral retinal detachment occurring at different ages. The patients also showed different extents of visual defects and diverse clinical manifestations, including cataract, iris–lens synechiae, inverted papillae, and ectopic foveas.

Conclusions: Our results expand the mutation spectrum of *VCAN* and further confirm that the splicing sites for exon 8 are mutation hot spots. Patients with WVR may present high phenotype variation; therefore, molecular analysis is very important for precise diagnosis of patients with inherited vitreoretinopathy.

Junwei Zhong and Jie Shi contributed equally to this work.

KEYWORDS
splicing variant, *VCAN*, versican transcripts, Wagner vitreoretinopathy

1 | INTRODUCTION

Wagner vitreoretinopathy (WVR, OMIM 143200), first described by Wagner in 1938, is a rare vitreoretinopathy that is transmitted in an autosomal dominant pattern (Adam et al., 2016). Patients with this disorder usually present with an optically empty vitreous due to massive liquefaction of the vitreous and preretinal avascular membrane during childhood or adolescence (Adam et al., 2016; Brézin et al., 2011; Meredith et al., 2007; Miyamoto et al., 2005; Mukhopadhyay et al., 2006). The other clinical features include presenile cataract, myopia, progressive chorioretinal degeneration or atrophy, and tractional or rhegmatogenous retinal detachment (Adam et al., 2016; Brézin et al., 2011; Meredith et al., 2007; Miyamoto et al., 2005; Mukhopadhyay et al., 2006). Relatively recent studies have revealed uveitis and congenital glaucoma as other clinical manifestations (Jewsbury et al., 2014; Rothschild, Audo, et al., 2013). Patients usually have different extents of visual defects (Adam et al., 2016; Brézin et al., 2011; Jewsbury et al., 2014; Meredith et al., 2007; Miyamoto et al., 2005; Mukhopadhyay et al., 2006; Rothschild, Audo, et al., 2013).

Wagner vitreoretinopathy is caused by disease-causing variants of the *VCAN* gene (MIM: 118661) (Miyamoto et al., 2005). This gene, also known as the *CSPG2* gene, is located at chromosome 5q14.2-q14.3 and contains 15 coding exons that encode versican, a large chondroitin sulfate proteoglycan (Miyamoto et al., 2005). Versican is an extracellular matrix protein and a constituent of the vitreous, where it plays a crucial role in maintaining the structural integrity of the vitreous (Islam & Watanabe, 2020). The versican protein structurally has three domains: two globular domains at the N- and C-terminals and chondroitin sulfate (CS) attachment domains in the central region (Islam & Watanabe, 2020). *VCAN* can express four different transcripts (V0, V1, V2, and V3) by alternative splicing of exons 7 and 8 with a different number of glycosaminoglycan (GAG) chains (Islam & Watanabe, 2020; Miyamoto et al., 2005). Isoform V0 has the both exons and contains 17–23 GAG chains, V1 lacks exon 7 and has 12–15 GAG chains, V2 lacks exon 8 and contains 5–8 GAG chains, and V3 lacks both exons 7 and 8 and has no GAG chains (Kloeckener-Gruissem et al., 2006).

At present, 34 *VCAN* variants have been reported based on the Human Gene Variant Database (HGMD) Professional 2021.4 and 18 of them cause WVR. The 18 variants included 12 different splice variants and six gross deletions (Ankala et al., 2018; Araújo et al., 2018; Brézin et al., 2011; Burin-des-Roziers et al., 2017; Chen et al., 2013; Jewsbury et al., 2014; Klee et al., 2021; Kloeckener-Gruissem et al., 2006, 2013; Li, Li, Sun, et al., 2020; Li, Li, Yang, et al., 2020; Meredith et al., 2007; Miyamoto et al., 2005; Mukhopadhyay et al., 2006; Ronan et al., 2009; Rothschild, Audo, et al., 2013; Rothschild, Brézin, et al., 2013). All the splicing effect variants have been located in the conserved exon 8 splice site (Ankala et al., 2018; Brézin et al., 2011; Chen et al., 2013; Jewsbury et al., 2014; Kloeckener-Gruissem et al., 2006, 2013; Meredith et al., 2007; Miyamoto et al., 2005; Mukhopadhyay et al., 2006; Ronan et al., 2009; Rothschild, Audo, et al., 2013; Rothschild, Brézin, et al., 2013), while the six gross deletions all involved exon 8 (Ankala et al., 2018; Burin-des-Roziers et al., 2017; Li, Li, Sun, et al., 2020). The pathogenic variants cause a partial or full deletion of exon 8, as well as imbalanced levels of versican isoforms.

In the current study, we reported a novel variant identified in four patients from a three-generation Chinese family initially diagnosed with family exudative vitreoretinopathy (FEVR). We used RT-PCR to compare the versican transcription patterns of the patients to those of normal controls, and we described the clinical features of our four patients.

2 | MATERIALS AND METHODS

2.1 | Patients

The study was approved by the Ethics Committee of the Beijing Tongren Hospital and followed the tenets of the Declaration of Helsinki. Four patients clinically diagnosed with FEVR from a three-generation Chinese family were referred to the Beijing Tongren Ophthalmic Center. The medical and family histories of the patients were well documented. All four patients underwent detailed ophthalmological examinations, including best-corrected visual acuity (BCVA) by Snellen E chart, slit-lamp biomicroscopy, indirect ophthalmoscopy under pupil dilatation, ocular B-ultrasonography, optical coherence tomography (OCT) scans, and fundus autofluorescence (FAF) evaluations (Heidelberg Engineering, Heidelberg, Germany).

2.2 | Targeted exome sequencing (TES)

After informed consent was obtained, peripheral blood samples were collected from all patients and their available family members, and genomic DNA was extracted from peripheral blood leukocytes using a genomic DNA extraction kit (Vigorous, Beijing, China), according to the manufacturer's protocol. We performed targeted exome sequencing (TES) in the proband using a capture panel that included 373 known inherited retinal degeneration genes. The Illumina library preparation and capture procedures were carried out as previously described (Sun et al., 2018).

2.3 | Bioinformatics analysis

The HGMD and LOVD databases were used to confirm known pathogenic variants. The pathogenicity of the variants was predicted by three in silico programs: PolyPhen2, Mutation Taster, and SIFT. Splice sites were predicted using ASSP, BDGP, NetGene2, ESEfinder 3.0, and MaxEntScan. The potential pathogenicity of the variants was classified according to the criteria described by the American College of Medical Genetics (ACMG) (Richards et al., 2015). Co-segregation analysis was performed in all family members whenever their DNA was available. Variant annotations were described according to the following transcript: *VCAN* NM_004385.

2.4 | RT-PCR analysis

Fresh anticoagulant peripheral blood samples (10 ml) were collected from the three patients in the families and from two normal controls. Lymphocytes were then isolated using Lymphocyte Separation Medium (Solarbio, Beijing, China). Total RNA was extracted from the lymphocytes with an RNAsimple Total RNA Kit (Tiangen, Beijing, China), followed by reverse transcription using FastKing cDNA Dispelling RT SuperMix (Tiangen, Beijing, China). The reverse-transcribed reaction included an initial step at 42°C for 15 min, followed by 95°C for 3 min. The cDNA was amplified with the four specific pairs of primers for the four known transcript isoforms of the *VCAN* described previously (Li, Li, Sun, et al., 2020). *GAPDH* primers were used as a control. The PCR fragments were electrophoresed in 2% agarose gel. Aberrant cDNA fragments were cut and purified with a TIANgel Midi Purification Kit (Tiangen, Beijing, China). Each gel-purified DNA band was confirmed by Sanger sequencing.

3 | RESULTS

3.1 | VCAN variant

TES analysis revealed a small heterozygous indel variant c.4004-4_c.4004-3delinsCA of the *VCAN* in the proband (Figure 1a). This variant has not previously been recorded in any public database. The novel variant was defined as uncertain, based on the ACMG guidelines and standards. Four of the five computational splice site algorithms predicted that the variant c.4004-4_c.4004-3delinsCA moderately reduced the normal splicing strength of intron 7 in *VCAN* (Table 1).

3.2 | Transcript analysis

The RT-PCT results from the lymphocytes revealed an abnormal *VCAN* transcript pattern and aberrant bands in transcripts V0 and V1 in three patients (Figure 1b,c). In the normal controls, the lymphocytes expressed isoforms V0, V1, and V3 but lacked V2 (Figure 1c). In the patients, the lymphocytes transcribed isoforms V0, V1, V2, and V3, and a short aberrant band was observed in isoforms V0 and V1 (Figure 1c). Sanger-DNA sequencing disclosed that the shortened transcripts lacked the first 39 nucleotides of the exon 8, indicating that the novel variant introduced a cryptic splicing site within exon 8, resulting in a 39 bp shortening of exon 8 (Figure 1d).

3.3 | Clinical findings

The three-generation pedigree had four affected members, suggesting an autosomal dominant inheritance mode (Figure 1a). Co-segregation analysis showed that all patients carried the novel variant c.4004-4_c.4004-3delinsCA. All patients had experienced retinal detachment in their childhood; however, none of them had nyctalopia complaints. The main clinical characteristics of each patient are summarized in Table 2.

The proband (III: 2) was a 3-year-old girl. She had been noted as being prone to falls during walking at 1 year of age. A dilated fundus examination revealed bilateral tractional retinal detachment (RD) without any retinal tears (RT). Due to her poor visual prognosis, observation was selected. At her latest examination in our clinic, she could not have a BCVA test due to her young age and her intraocular pressure (IOP) was normal. A slit-lamp examination showed normal anterior segments and mild opacities of the lenses. Fundus examination exhibited relatively stable tractional RD (Figure 2a). No RT was observed after

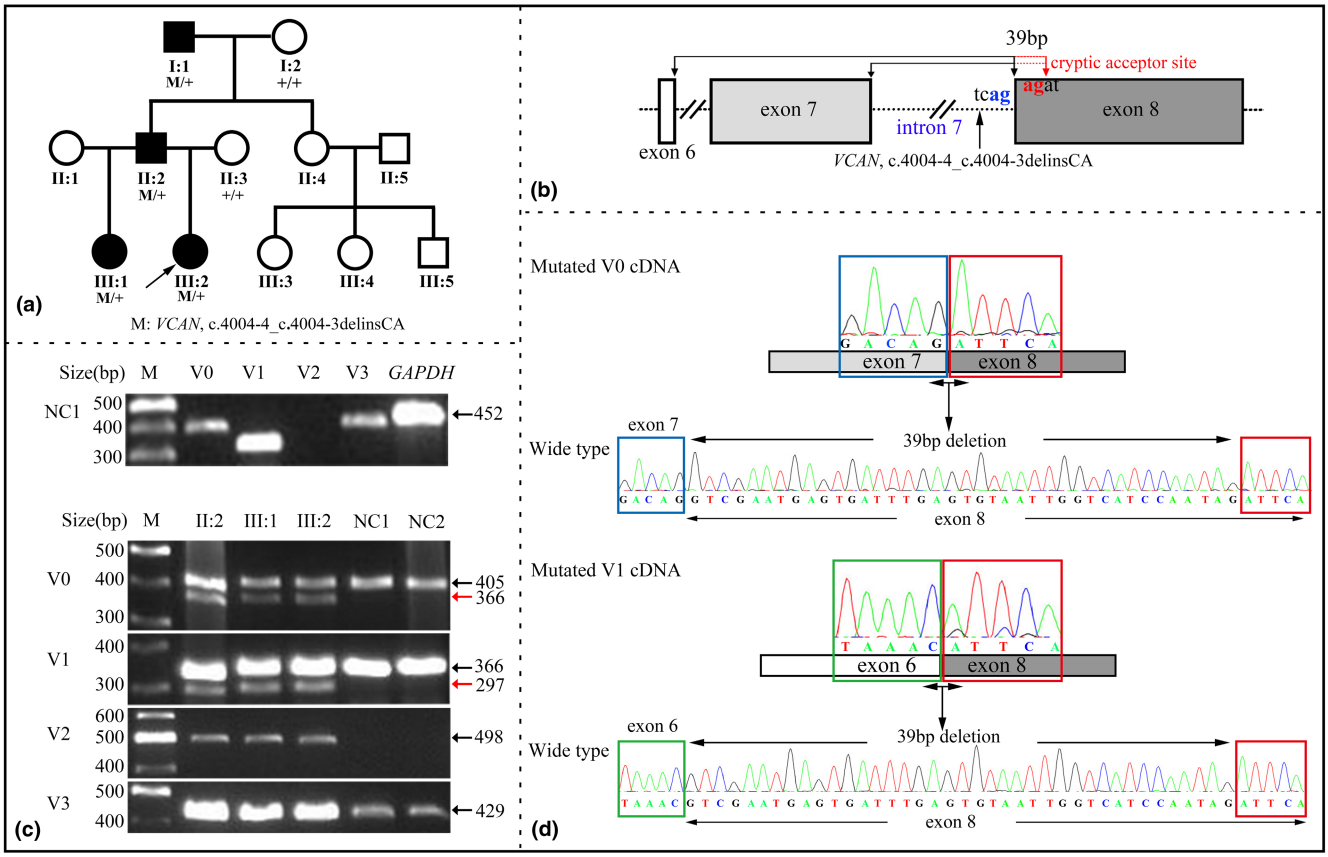

FIGURE 1 Pedigree, co-segregation for the novel variant c.4004-4_c.4004-3delinsCA in the family with vitreoretinopathy, and Versican (*VCAN*) transcript analysis. (a) Pedigree, co-segregation for the novel variant c.4004-4_c.4004-3delinsCA in the family with vitreoretinopathy. (b) Schematic diagram shows the position of the novel variant and the cryptic acceptor site. (c) Agarose gel electrophoresis displays the RT-PCR products for V0–V3 of the *VCAN* mRNA transcripts and the mRNA of *GAPDH* from lymphocytes of a normal control (NC). Agarose gel electrophoresis displays the RT-PCR products for V0–V3 of the *VCAN* mRNA transcripts in the three patients and the normal controls. (d) Partial sequence chromatogram of this aberrant V0 and V1transcripts lacking the first 39 bp of VCAN exon 8.

careful examination. Ocular B-ultrasonography revealed vitreous opacities and RD (Figure 2b). The axial length was 19.0 mm in both eyes.

The proband's 36-year-old father (II: 2) had undergone multiple ocular surgeries. He had suffered a sudden visual acuity loss in the left eye at age 9 after a crush injury. His BCVA was 1.5 OD and no light perception (NLP) OS. An ocular examination revealed severe vitreous hemorrhage and RD in the left eye. He underwent pars plana vitrectomy (PPV) and pneumatic retinopexy. Postoperatively, his RD receded and his VA in the OS was 0.02; however, the RD reoccurred at the 1-year follow-up visit and his vision reduced to LP. No further surgical intervention was performed due to the poor visual function outcome. He had experienced a sudden vision reduction in the OD at age 20. An ocular examination had revealed rhegmatogenous RD in the OD, and he had received PPV and silicon oil tamponade injection. He had then received multiple surgical procedures, including removal of the silicon oil, cataract extraction, and intraocular lens implantation at age 21. Postoperatively, his RD receded, and the VA in the OD was 0.4. Recurrent RD in the OD was found at age 30, and he underwent PPV and silicon oil tamponade again. The retina remained reattached after the surgery, with BCVA 0.2 in the right eye. At his latest examination at our eye center, his BCVA was 0.05 OD and LP OS. Iris–lens synechiae, iris atrophy, and opacities of the lenses were observed in both eyes, and an ectopic intraocular lens was found in his right eye (Figure 2c). His fundi were invisible due to the dense cataracts in both eyes and his ocular B-ultrasonography showed dense vitreous opacity after silicon oil tamponade in the right and a complete RD in the left eye (Figure 2d).

The proband's 10-year-old sister (III:1) had blurred vision in her right eye at the age of eight. A fundus examination revealed bilateral rhegmatogenous RD in the inferotemporal quadrant peripheral retina. She underwent scleral buckle and cryoretinopexy surgeries in both eyes at another hospital, and her retina remained attached at the 2-year follow-up visit. At her latest examination

TABLE 1 Prediction of the published and novel *VCAN* splice-site variants by in silico analyses

Sequence	Position/function	ASSP	BDGP	Netgene2	ESEfinder	MaxEnt-scan	Experimental mRNA confirmation	Source
VCAN (NM_004385) wild type	Intron 7/acceptor	13.348	0.99	0.97	12.2299	9.88		
c.4004−1G>C	Intron 7/acceptor	3.873	–	–	–	1.82	Yes	Kloeckener-Gruissem et al. (2013)
c.4004−1G>A	Intron 7/acceptor	2.873	–	–	–	1.13	Yes	Mukhopadhyay et al. (2006)
c.4004−1G>T	Intron 7/acceptor	-	–	–	–	1.29	No	Chen et al. (2013)
c.4004−2A>G	Intron 7/acceptor	2.386	–	–	–	1.93	Yes	Miyamoto et al. (2005)
c.4004−2A>T	Intron 7/acceptor	2.386	–	–	–	1.52	Yes	Brézin et al. (2011)
c.4004-4_c.4004-3delinsCA	Intron 7/acceptor	9.892	0.95	0.33	8.8261	7.37	Yes	This study
c.4004−5T>C	Intron 7/acceptor	12.739	0.99	0.94	11.8009	8.14	Yes	Mukhopadhyay et al. (2006)
c.4004−5T>A	Intron 7/acceptor	10.731	0.97	0.83	9.7756	7.7	Yes	Mukhopadhyay et al. (2006)
c.4004−6T>A	Intron 7/acceptor	10.857	0.95	0.43	–	7.83	No	Rothschild, Brézin, et al. (2013)
VCAN (NM_004385) wild type	Intron 8/donor	13.544	1	1	10.4778	10.77		
c.9265+1G>A	Intron 8/donor	–	–	–	–	2.58	Yes	Rothschild, Audo, et al. (2013)
c.9265+1G>T	Intron 8/donor	–	–	–	–	2.26	No	Ronan et al. (2009)
c.9265+1G>C	Intron 8/donor					2.49	No	Klee et al. (2021)
c.9265+2T>A	Intron 8/donor	–	–	–	–	2.58	Yes	Kloeckener-Gruissem et al. (2013)

TABLE 2 The clinical features of the four patients in the family

Patient	Gender/ age (y)	BCVA OD/OS	Iris–lens synechiae	Cataract	Glaucoma	Vitreous opacity	RD	Chorioretinal atrophy	Additional features
I:1	M/71	NA/LP	No	Yes	Yes	Yes	Yes	Yes	–
II:2	M/36	0.05/LP	Yes	Yes	No	Yes	Yes	NA	NA
III:1	F/10	1.0/0.3	No	No	No	Yes	Yes	Yes	EF and IP
III:2	F/3	NA	No	Yes	No	Yes	Yes	No	–

Abbreviations: BCVA, best-corrected visual acuity; EF, ectopic foveas; IP, inverted papilla; LP, light perception; NA, not available; OD, right eye; OS, left eye; RD, retinal detachment; y, years.

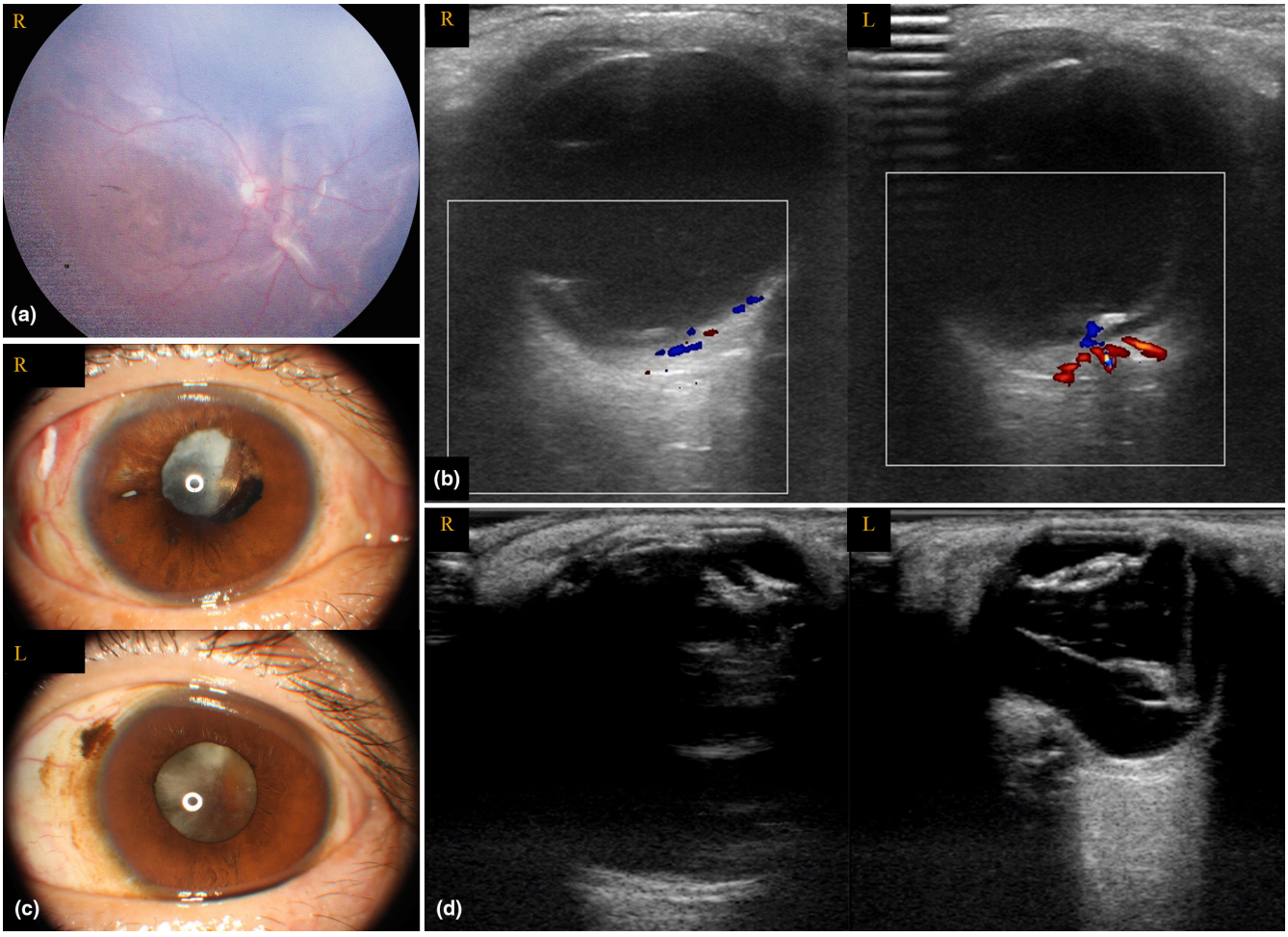

FIGURE 2 Fundus photographs (FP), ocular B-ultrasonography, and anterior segment photographs (ASP) of the proband and her father. (a) FP of the proband's right eye shows retinal detachment (RD). (b) Her ocular B-ultrasonography shows bilateral RD and vitreous opacity or strands. (c) ASPs of the proband's father exhibit pupil synechiae, iris atrophy, and opacities of the lenses in both eyes, ectopic IOL in his right eye. (d) His ocular B-ultrasonography shows dense vitreous opacity after silicon oil tamponade in the right eye and a complete RD in the left eye.

at our eye center, her BCVA was 1.0 OD and 0.3 with refraction -2.00CX155 OS. A slit-lamp examination showed normal anterior segments. A fundus examination revealed inverted papilla, ectopic foveas, vitreous veils, and mild RPE mottling in the mid-periphery retina (Figure 3a). A mild dragging of the retinal vasculature from the disk was observed in the right eye, while macular atrophy, retinoschisis, and fibrotic proliferative members were found in the left eye (Figure 3a). FAF revealed an abnormal hypo- or hyper-autofluorescence pattern in the central retina (Figure 3b). SD-OCT examination revealed dense vitreous and vitreous veils in both eyes (Figure 3c). Retinoschisis and outer retinal tubulations, small cystoid cavities, and atrophy at the

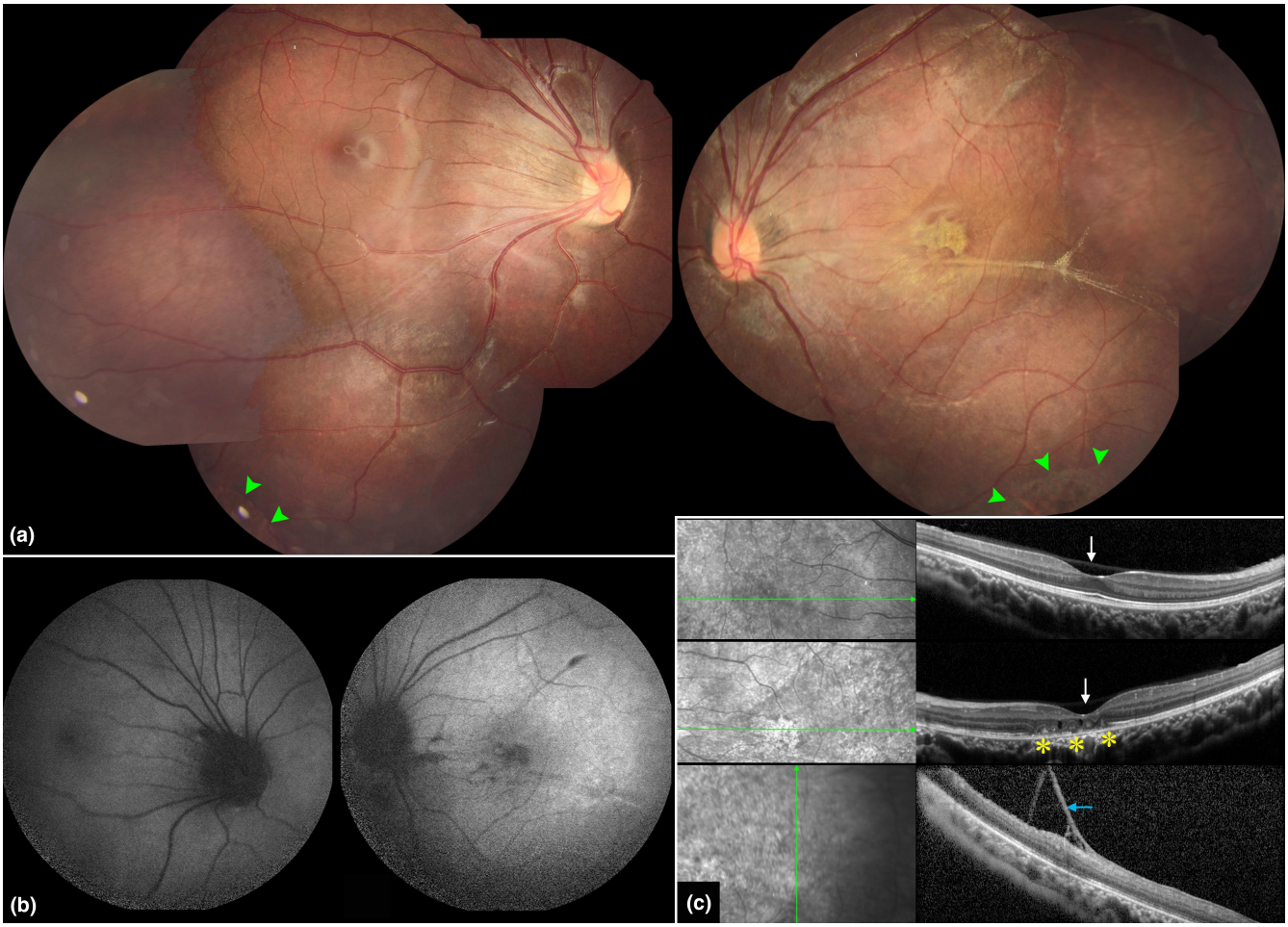

FIGURE 3 Fundus photographs (FP), fundus autofluorescence (FAF), and OCT images of the proband's sister. (a) FPs show an inverted papilla, ectopic foveas, vitreous veils, mild RPE mottling in the mid-periphery retina, and demarcated chorioretinal atrophy in the peripheral retina (green arrowhead). (b) FAF displays relatively normal autofluorescence pattern in the right eye and abnormal hyper-autofluorescence in the left eye. (c) OCT images show a dense posterior hyaloid forming a bridge over the foveal pit (white arrow) in both eyes and retinoschisis and outer retinal tubulations at the macula (yellow asterisk), and a vitreous veil in the left eye (blue arrow).

macula were observed in the left eye (Figure 3c). Her ERG recordings were relative normal in her right eye and mild decreased rod function as well as severe decreased cone function in her left eye.

The proband's 71-year-old grandfather (I:1) suffered profound visual defect in the right eye since his childhood without ocular examination. He had received cataract extraction and intraocular lens implantation in the left eye at age 50 at another hospital. Postoperatively, his VA in the OS was 0.6. He experienced obvious visual blurring in his left eye 4 months ago. B-ultrasonography showed dense vitreous opacity and RD in both eyes. He then underwent the right eye ball enucleating due to corneal epithelial and stromal edema and uncontrollable elevated IOP at another hospital. At his latest examination at our eye center, his VA in the OS was LP. Fundus examination revealed vitreous opacity and rhegmatogenous RD. He would accept PPV in his local hospital based on our recommendation.

4 | DISCUSSION

This study described a novel splice variant c.4004--4_c.4004-3delinsCA of the *VCAN* identified in a Chinese family initially suspected of having FEVR. We also demonstrated by RT-PCR analysis that this novel variant caused unbalanced alternative splicing in the pathogenesis of WVR.

At present, only 18 distinct disease-causing variants of the *VCAN* have been reported, and 12 of them are splicing effect variants involving exon 8 (Table 1). The novel variant c.4004-4_c.4004-3delinsCA reported here is located in the third and fourth positions of the acceptor splice site of intron 7, which are not the canonical acceptor splicing sites of intron 7. According to in silico analysis, the novel variant has less of a decrease in splicing strength than observed with variants in the canonical acceptor splicing site of intron 7, but the predicted values were consistent with the values of the variants located in

the fifth and sixth sites. Despite this smaller decrease in strength, our mRNA analysis of the patients verified that the novel variant caused an abnormal splicing of exon 8 and an expression shift in the *VCAN* isoforms. Our mRNA analysis results were similar to those reported for other variants residing at the acceptor splicing site of intron 7 (Brézin et al., 2011; Miyamoto et al., 2005; Mukhopadhyay et al., 2006; Rothschild, Audo, et al., 2013). Our results further suggest that the variant effects on splicing predicted by in silico analysis might be underestimated. Therefore, mRNA analysis is essential for variants not occurring at the canonical splicing sites, which usually are AG or GT sequences at the 3′ and 5″ splice sites.

The product of *VCAN* gene expression is versican, a large chondroitin sulfate (CS) proteoglycan that is secreted and incorporated into the extracellular matrix (Islam & Watanabe, 2020). It has four different classical isoforms created by alternative splicing of exon7 and exon8; these exons encode GAG-attachment domains GAGα and GAGβ (Islam & Watanabe, 2020; Miyamoto et al., 2005). Expression patterns of each isoform varied among human tissues: V1 and V3 variants were relatively widespread, whereas V0 and V2 showed tissue-specifically transcribed, such as adult whole brain expressed only V2, while heart organ expressed V0, V1, and V3 (Miyamoto et al., 2005). Human retina expressed all the isoforms, with relatively high expression of the V0 and V3 isoforms (Miyamoto et al., 2005). Compare to expression pattern (V0, V1, and V3) observed in the normal lymphocytes, the lymphocytes of the patients in this pedigree expressed all the four isoforms, which was consistent with previous observation (Mukhopadhyay et al., 2006). Due to the difference of mRNA transcript of *VCAN* in human tissue, we could not predict how this novel variant affected VCAN expression in the retina. Similar to the reported variants at the acceptor splicing site of intron 7, the novel variant also led to skipping of exon 8 or a deletion of 39 base pairs (bp) (Brézin et al., 2011; Miyamoto et al., 2005; Mukhopadhyay et al., 2006; Rothschild, Audo, et al., 2013). The 39 bp sequence encodes 13 amino acids located at the start of the GAGβ chain (VCAN p.1335-1347). These 13 residues do not contain any GAG-attachment sites, but they are highly conserved among mammals, implying their significance for the structure and function of versican. A recent structural bioinformatics study by Tang et al. (2019) identified a novel putative matrix metalloproteinase (MMP) cleavage site within the deletion region. Those authors speculated that the elimination of this MMP site due to the 13 residue deletion could affect proteolytic processing of versican and its interactions with its binding partners in the vitreous.

The four patients in this family all had vitreous strands or veils and RD, which are the typical clinical features of WVR (Adam et al., 2016; Brézin et al., 2011; Jewsbury et al., 2014; Meredith et al., 2007; Miyamoto et al., 2005; Mukhopadhyay et al., 2006; Rothschild, Audo, et al., 2013). RD is the main reason for visual impairment in patients with WVR and is usually caused by contraction of the vitreous strands or the preretinal membranes. Although all four patients carried the same pathogenic variant, their onset ages for RD differed. The proband had bilateral tractional RD at 1 year of age, while her father and sister experienced rhegmatogenous RD at about age 8 or 9 years, which was close to the average onset age of 9.5 years for RD reported in previous studies (Adam et al., 2016). This implies that other environmental or genetic modifiers are probably involved.

The proband was initially misdiagnosed with FVER, which is another relatively common inherited vitreoretinopathy (Adam et al., 2016; Edwards, 2008). The highly variable phenotypes make WVR diagnosis particularly challenging, especially in younger children who cannot undergo full fundus examinations. For this reason, molecular analysis is very useful for providing an accurate diagnosis. An accurate diagnosis of WVR can be valuable for genetic counseling while also identifying patients at risk of RD or patients with asymptomatic RD. The proband's father presented bilateral iris–lens synechiae, but whether his iris–lens synechiae were due to a primary anterior uveitis or a secondary result from his multiple surgical interventions is difficult to ascertain. None of the four patients had a night blindness complaint; however, patient III:1 (the sister of the proband) showed demarcated chorioretinal atrophy in her peripheral retina. The chorioretinal atrophy observed in patients with WVR progresses with aging (Adam et al., 2016); therefore, we intend to follow up this patient in the future.

We did not perform quantitative RT-PCR for the *VCAN* transcript in the three patients, and this is one limitation of this study. However, previous studies have indicated that the expression level for different versican isoforms in blood cells or skin fibroblasts was not related to patient phenotype (Kloeckener-Gruissem et al., 2006; Mukhopadhyay et al., 2006). Another limitation is the small number of patients in this family.

In conclusion, our results expand the mutation spectrum of *VCAN* and further confirm that the splicing sites in exon 8 are mutation hot spots. Patients with WVR may present high phenotype variation; therefore, molecular analysis is very important for precise diagnosis of patients with WVR.

AUTHOR CONTRIBUTIONS

JZ contributed in study design, sequencing, RT-PCR experiments, data analysis, and manuscript preparation. JS participated in sequencing, RT-PCR experiments, and

data analysis. XZ contributed in providing clinical examinations. KX, XZ, and YX participated in data collection and sequencing. YL contributed in the study design, checking the data, revising the manuscript critically, and funding. All authors approved the final version.

ACKNOWLEDGMENTS

This study was supported by the National Key R&D Program of China (2016YFC0905200). The funding organizations had no role in designing or conducting this research.

CONFLICT OF INTEREST

No authors have any financial/conflicting interests to disclose.

ETHICS STATEMENT

The study was approved by the Ethics Committee of the Beijing Tongren Hospital and followed the tenets of the Declaration of Helsinki. Written informed consent was obtained from the participants or their parents.

DATA AVAILABILITY STATEMENT

The data that support the findings of this study are available from the corresponding author upon reasonable request.

ORCID

Junwei Zhong https://orcid.org/0000-0002-7297-7684

REFERENCES

Adam, M. P., Ardinger, H. H., Pagon, R. A., Wallace, S. E., Bean, L. J. H., Gripp, K. W., Mirzaa, G. M., & Amemiya, A. (2016). VCAN-related vitreoretinopathy. In M. P. Adam, H. H. Ardinger, R. A. Pagon, S. E. Wallace, L. J. H. Bean, K. W. Gripp, G. M. Mirzaa, & A. Amemiya (Eds.), *GeneReviews®*. University of Washington.

Ankala, A., Jain, N., Hubbard, B., Alexander, J. J., & Shankar, S. P. (2018). Is exon 8 the most critical or the only dispensable exon of the VCAN gene? Insights into VCAN variants and clinical spectrum of Wagner syndrome. *American Journal of Medical Genetics: Part A*, *176*, 1778–1783. https://doi.org/10.1002/ajmg.a.38855

Araújo, J. R., Tavares-Ferreira, J., Estrela-Silva, S., Rocha, P., Brandão, E., Faria, P. A., Falcão-Reis, F., & Rocha-Sousa, A. (2018). WAGNER syndrome: Anatomic, functional and genetic characterization of a Portuguese family. *Graefe's Archive for Clinical and Experimental Ophthalmology*, *256*, 163–171. https://doi.org/10.1007/s00417-017-3800-0

Brézin, A. P., Nedelec, B., Barjol, A., Rothschild, P. R., Delpech, M., & Valleix, S. (2011). A new VCAN/versican splice acceptor site mutation in a French Wagner family associated with vascular and inflammatory ocular features. *Molecular Vision*, *17*, 1669–1678.

Burin-des-Roziers, C., Rothschild, P. R., Layet, V., Chen, J. M., Ghiotti, T., Leroux, C., Cremers, F. P., Brézin, A. P., & Valleix, S. (2017). Deletions overlapping VCAN exon 8 are new molecular defects for Wagner disease. *Human Mutation*, *38*, 43–47. https://doi.org/10.1002/humu.23124

Chen, X., Zhao, K., Sheng, X., Li, Y., Gao, X., Zhang, X., Kang, X., Pan, X., Liu, Y., Jiang, C., Shi, H., Chen, X., Rong, W., Chen, L. J., Lai, T. Y., Liu, Y., Wang, X., Yuan, S., Liu, Q., … Zhao, C. (2013). Targeted sequencing of 179 genes associated with hereditary retinal dystrophies and 10 candidate genes identifies novel and known mutations in patients with various retinal diseases. *Investigative Ophthalmology & Visual Science*, *54*, 2186–2197. https://doi.org/10.1167/iovs.12-10967

Edwards, A. O. (2008). Clinical features of the congenital vitreoretinopathies. *Eye (London, England)*, *22*, 1233–1242. https://doi.org/10.1038/eye.2008.38

Islam, S., & Watanabe, H. (2020). Versican: A dynamic regulator of the extracellular matrix. *The Journal of Histochemistry and Cytochemistry*, *68*, 763–775. https://doi.org/10.1369/0022155420953922

Jewsbury, H., Fry, A. E., Watts, P., Nas, V., & Morgan, J. (2014). Congenital glaucoma in Wagner syndrome. *Journal of AAPOS*, *18*, 291–293. https://doi.org/10.1016/j.jaapos.2013.12.014

Klee, E. W., Cousin, M. A., Pinto E Vairo, F., Morales-Rosado, J. A., Macke, E. L., Jenkinson, W. G., Ferrer, A., Schultz-Rogers, L. E., Olson, R. J., Oliver, G. R., Sigafoos, A. N., Schwab, T. L., Zimmermann, M. T., Urrutia, R. A., Kaiwar, C., Gupta, A., Blackburn, P. R., Boczek, N. J., Prochnow, C. A., … Lazaridis, K. N. (2021). Impact of integrated translational research on clinical exome sequencing. *Genetics in Medicine*, *23*, 498–507.

Kloeckener-Gruissem, B., Bartholdi, D., Abdou, M. T., Zimmermann, D. R., & Berger, W. (2006). Identification of the genetic defect in the original Wagner syndrome family. *Molecular Vision*, *12*, 350–355.

Kloeckener-Gruissem, B., Neidhardt, J., Magyar, I., Plauchu, H., Zech, J. C., Morlé, L., Palmer-Smith, S. M., Macdonald, M. J., Nas, V., Fry, A. E., & Berger, W. (2013). Novel VCAN mutations and evidence for unbalanced alternative splicing in the pathogenesis of Wagner syndrome. *European Journal of Human Genetics*, *21*, 352–356. https://doi.org/10.1038/ejhg.2012.137

Li, H., Li, H., Yang, L., Sun, Z., Wu, S., & Sui, R. (2020). Clinical and genetic study on two Chinese families with Wagner vitreoretinopathy. *Ophthalmic Genetics*, *41*, 432–439. https://doi.org/10.1080/13816810.2020.1786843

Li, S., Li, M., Sun, L., Zhao, X., Zhang, T., Huang, L., Huang, S., Chen, C., Wang, Z., & Ding, X. (2020). Identification of novel copy number variations of VCAN gene in three Chinese families with Wagner disease. *Genes (Basel)*, *11*, 992. https://doi.org/10.3390/genes11090992

Meredith, S. P., Richards, A. J., Flanagan, D. W., Scott, J. D., Poulson, A. V., & Snead, M. P. (2007). Clinical characterisation and molecular analysis of Wagner syndrome. *The British Journal of Ophthalmology*, *91*, 655–659. https://doi.org/10.1136/bjo.2006.104406

Miyamoto, T., Inoue, H., Sakamoto, Y., Kudo, E., Naito, T., Mikawa, T., Mikawa, Y., Isashiki, Y., Osabe, D., Shinohara, S., Shiota, H., & Itakura, M. (2005). Identification of a novel splice site mutation of the CSPG2 gene in a Japanese family with Wagner syndrome. *Investigative Ophthalmology & Visual Science*, *46*, 2726–2735. https://doi.org/10.1167/iovs.05-0057

Mukhopadhyay, A., Nikopoulos, K., Maugeri, A., de Brouwer, A. P., van Nouhuys, C. E., Boon, C. J., Perveen, R., Zegers, H. A., Wittebol-Post, D., van den Biesen, P. R., van der Velde-Visser, S. D., Brunner, H. G., Black, G. C., Hoyng, C. B., & Cremers, F. P. (2006). Erosive vitreoretinopathy and Wagner disease are caused by intronic mutations in CSPG2/Versican that result in an imbalance of splice variants. *Investigative Ophthalmology & Visual Science*, *47*, 3565–3572. https://doi.org/10.1167/iovs.06-0141

Richards, S., Aziz, N., Bale, S., Bick, D., Das, S., Gastier-Foster, J., Grody, W. W., Hegde, M., Lyon, E., Spector, E., Voelkerding, K., Rehm, H. L., & ACMG Laboratory Quality Assurance Committee. (2015). Standards and guidelines for the interpretation of sequence variants: A joint consensus recommendation of the American College of Medical Genetics and Genomics and the Association for Molecular Pathology. *Genetics in Medicine*, *17*, 405–424. https://doi.org/10.1038/gim.2015.30

Ronan, S. M., Tran-Viet, K. N., Burner, E. L., Metlapally, R., Toth, C. A., & Young, T. L. (2009). Mutational hot spot potential of a novel base pair mutation of the CSPG2 gene in a family with Wagner syndrome. *Archives of Ophthalmology*, *127*, 1511–1519.

Rothschild, P. R., Audo, I., Nedelec, B., Ghiotti, T., Brézin, A. P., Monin, C., & Valleix, S. (2013). De novo splice mutation in the versican gene in a family with Wagner syndrome. *JAMA Ophthalmology*, *131*, 805–807. https://doi.org/10.1001/archophthalmol.2009.273

Rothschild, P. R., Brézin, A. P., Nedelec, B., Burin des Roziers, C., Ghiotti, T., Orhant, L., Boimard, M., & Valleix, S. (2013). A family with Wagner syndrome with uveitis and a new versican mutation. *Molecular Vision*, *19*, 2040–2049.

Sun, T., Xu, K., Ren, Y., Xie, Y., Zhang, X., Tian, L., & Li, Y. (2018). Comprehensive molecular screening in Chinese usher syndrome patients. *Investigative Ophthalmology & Visual Science*, *59*, 1229–1237. https://doi.org/10.1167/iovs.17-23312

Tang, P. H., Velez, G., Tsang, S. H., Bassuk, A. G., & Mahajan, V. B. (2019). VCAN canonical splice site mutation is associated with vitreoretinal degeneration and disrupts an MMP proteolytic site. *Investigative Ophthalmology & Visual Science*, *60*, 282–293. https://doi.org/10.1167/iovs.18-25624

How to cite this article: Zhong, J., Shi, J., Zhang, X., Xu, K., Zhang, X., Xie, Y., & Li, Y. (2023). A novel splicing variant of *VCAN* identified in a Chinese family initially diagnosed with familial exudative vitreoretinopathy. *Molecular Genetics & Genomic Medicine*, *11*, e2083. https://doi.org/10.1002/mgg3.2083